Study of Pulse Electrochemical Machining Characteristics of Spheroidal Cast Iron Using Sodium Nitrate Electrolyte

O. Weber[1], D. Bähre[2], A. Rebschläger[1]
[1]Center for Mechatronics and Automatization, Saarbrücken, Germany
[2]Institute of Production Engineering, Saarland University, Saarbrücken, Germany

Abstract
In this contribution, the potential of Pulse Electrochemical Machining (PECM) for the machining of spheroidal cast iron is investigated with regard to the machining performance during electrolysis with sodium nitrate as electrolyte and stainless steel as cathode. Therefore, the material removal characteristics of spheroidal cast iron with PECM are determined by performing systematic design of experiments techniques applying an industrial PECM machine system (PEMCenter8000) to fulfil the effective utilization of the process and to minimize the number of trials. An analysis of the precision of the manufactured geometries and the possibility of generating defined surface qualities are contents of this study. Suggestions for the process design are derived from these results and a concept for the future modelling is presented.

Keywords
Pulse Electrochemical Machining (PECM), Cast Iron, Response Surface Methodology (RSM)

1 INTRODUCTION

Pulse Electrochemical Machining (PECM) is an unconventional procedure combining pulsed current and pulsed electrode feed rate (Figure 1), which is very suitable for high precision production in series manufacturing. The main advantage compared to conventional electrochemical processes is that the current pulse is only triggered at the bottom dead centre. This allows for reaching smaller gaps compared to other electrochemical processes, leading to more accuracy. Besides, the electrolyte in the interelectrode gap is refreshed by a removal product free electrolyte during the pulse off-time leading to better process stability.

Different applications require the positioning of complex geometric contours with high precision and high surface quality demands in work pieces made of cast iron. Valve seats in pump bodies, e.g., are required for high pressure fuel injection and other hydraulic applications. Traditional machining of spheroidal cast iron by cutting causes normally serious tool wear. Because of its non-tool wear properties, PECM appears as an economically very attractive alternative procedure.

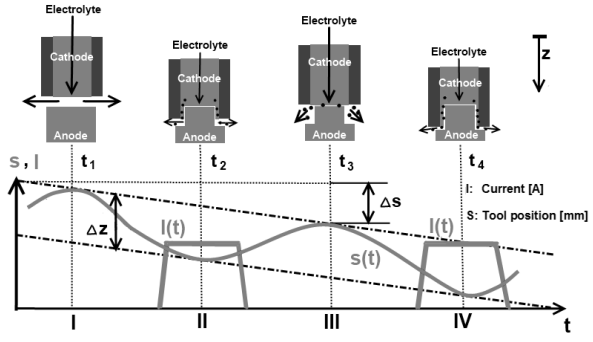

Figure 1 - Pulse Electrochemical Machining principle

Although a few attempts of understanding the mechanisms of the pulse electrochemical machining process have been reported [1], [2], the current models and analysis of the machining characteristics of spheroidal cast iron are not sufficient to satisfy the issues and challenges industrials are confronted with.

Therefore, the present paper emphasizes features of the development of comprehensive empirical mathematical models for correlating the interactive and higher-order influences of the various machining parameters (applied voltage, pulse on-time, vibration frequency of the tool, feed rate and electrolyte pressure) on the metal removal rate (MRR) and surface roughness (R_a), for achieving controlled PECM and optimal selection of process parameters in order to reduce the product development phase. The investigations into the influence of these parameters have been carried out by developing mathematical models based on the Response Surface Methodology (RSM) [3].

2 EXPERIMENTAL SET-UP

The chemical composition of the used spheroidal cast iron is shown in Table 1.

C	*Si*	*Mn*	*S*	*Cr*	*Cu*	*Ni*	*Fe*
3.6	2.3	0.5	0.01	0.05	0.5	0.06	balance

Table 1 - Spheroidal cast iron composition

The dimensions of the tube-shaped specimens were 19mm in diameter and 30mm in height. They were drilled by a central hole of 7mm in diameter which

enables an inside-out electrolyte flushing. All samples were grinded before the measuring to maintain the surface roughness R_a=0.8µm. The working surface of the cathode made of stainless steel had been electrochemically machined in advance to provide for the roughness R_a=0.1µm. The experiments were conducted on an industrial PEMCenter8000 from the company PEMTec SNC in Forbach (France). The electrolyte was axially fed to the processing zone through the workpiece. The electrolyte used for the experiments was a solution of $NaNO_3$ with a concentration of 8%, a conductivity of 65mS/cm and was maintained to 21°C during the investigations. The machining was carried out for a fixed time interval of 120s and an initial working gap of 30µm. The material removal rate was determined by measuring the mass loss on a precision balance from the company Sartorius and the surface roughness with a profilometer MarSurf XR/XT 20.

3 DESIGN OF EXPERIMENTS

The design of experiments used for analyzing the influence of the fundamental process parameters (applied voltage, pulse on-time, tool vibration frequency, feed rate and electrolyte pressure) on the machining characteristics (MRR and R_a) is proposed according to Siebertz, Bebber and Hochkirchen [4]. The experimentation scheme consists of a central composite second order design with a 2^k factorial, in which *k* is the number of parameters, with the aim to study both the higher-order parameter effects and their interactions.

For those five process variables, the design requires 52 experiments subdivided in 32 factorial points, 10 axial points corresponding to the central composite design and 10 centre points for replication to estimate the experimental error. The experimental plan was generated and analyzed with the statistical software Minitab 16. The central composite parameter α was set to 2.37841 to ensure a rotatable design and the 10 central points guarantee uniform precision for the developed mathematical models.

The original values of experimental parameters in this set of trials are shown in Table 2. The parameter levels were chosen so that each parameter combination of the experimental plan provides for a stable process. The experiments have been carried out according to the designed experimentation based on the central composite second-order rotatable design with uniform precision as presented in Table 3.

4 RESPONSE SURFACE METHODOLOGY

Response Surface Methodology (RSM) is a procedure for analyzing the relationship between the process variables and the responses. These are mathematically fitted by second-order polynomials which enable the evaluation of the parametric effects of the process parameters and their interactions on the investigated machining criteria. Those polynomials can be developed as follows:

$$Y = b_0 + \sum_{i=1}^{k} b_i \cdot X_i + \sum_{i=1}^{k} b_{ii} \cdot X_i^2 + \sum_{i \neq j}^{k} b_{ij} \cdot X_i \cdot X_j \quad (1)$$

Y represents the corresponding response and X_i are coded levels of quantitative variables. The coefficient b_0 is the constant term and the coefficients b_i, b_{ii}, and b_{ij} are respectively the linear, quadratic and interaction terms estimated by applying the least square technique using the observations collected through the design points.

4.1 Mathematical modelling of MRR

Based on Eq. (1) and using the results presented in Table 3, the mathematical relationship for correlating the MRR (in g/min) and the considered process parameters was obtained as follows:

$$MRR = 0.2004 + 0.0214X_1 + 0.0056X_2 + 0.0034X_3 + 0.0464X_4 + 0.0040X_5 - 0.0041X_1^2 - 0.0008X_2^2 + 0.0030X_3^2 + 0.0051X_4^2 + 0.0029X_5^2 + 0.0025X_1X_2 + 0.0002X_1X_3 - 0.0008X_1X_4 - 0.0001X_1X_5 + 0.0007X_2X_3 - 0.0038X_2X_4 - 0.0004X_2X_5 - 0.0011X_3X_4 + 0.0001X_3X_5 - 0.0020X_4X_5 \quad (2)$$

4.2 Mathematical modelling of R_a

A comprehensive model based on Eq. (1) has been developed to correlate the interaction and higher-order effects of the previously mentioned process parameters on the R_a criteria (in µm). The mathematical relationship obtained for analyzing the influences of the dominant machining parameters is given by:

$$R_a = 6.4568 + 0.1325X_1 + 0.2952X_2 + 0.2751X_3 - 1.0994X_4 - 0.1583X_5 + 0.1909X_1^2 + 0.0735X_2^2 + 0.0929X_3^2 + 0.3932X_4^2 - 0.0742X_5^2 + 0.1681X_1X_2 + 0.2215X_1X_3 + 0.2557X_1X_4 - 0.0001X_1X_5 - 0.1105X_2X_3 - 0.0714X_2X_4 + 0.0953X_2X_5 + 0.1375X_3X_4 - 0.0899X_3X_5 - 0.0033X_4X_5 \quad (3)$$

Parameters	Symbol	Levels				
		-α / -2.37841	-1	0	1	α / 2.37841
Voltage (V)	X_1	6.2	9	11	13	15.8
Pulse on-time (ms)	X_2	2.1	2.9	3.5	4.1	4.9
Frequency (Hz)	X_3	40.5	46	50	54	59.5
Feed rate (mm/min)	X_4	0.015	0.07	0.11	0.15	0.205
Pressure (bar)	X_5	1.12	2.50	3.50	4.50	5.88

Table 2 - Original values of experimental parameters and their coded levels

5 ANALYSIS OF THE DEVELOPED MODELS

The analysis of variance (ANOVA) and the F-ratio test have been performed to justify the goodness of the mathematical modelled fittings. The calculated values of F-ratio for lack of fit are compared to the critical Fisher value for a 95% confidence limit and the corresponding degrees of freedom. As shown in Table 4, the F-values for lack of fit for MRR (2.02) and R_a (2.52) are smaller than the critical Fisher value ($F_{(0.05;22;9)}$=2.92), indicating that the model is considered as statistically significant. Besides, the obtained R-square coefficients for both MRR and R_a are about 97%, ensuring an excellent fitting for the relationship between the process parameters and the investigated machining criteria. Finally, the calculated models were tested and confirmed by applying the student's *t*-test (Table 5). The obtained values are smaller than the unilateral critical student t-value for a 95% confidence limit and the corresponding degrees of freedom ($t_{(0.05;31)}$=1.70). In conclusion, the models are adequate and demonstrate the independent, quadratic and interactive effects of the considered machining parameters on MRR and R_a criteria. However, these models and the results presented in the next paragraph are only valid for the process conditions presented in paragraph 2 and the parameter field listed in Table 2.

6 RESULTS AND DISCUSSION

6.1 Effect of machining parameters on MRR

The mathematically developed model given by Eq. (2) enables the quantitative analysis of the considered process parameters on the MRR behaviour. The contour plots - Figures 2 and 3 - were drawn for various combinations. The numbers represented are MRR values. The parameters not investigated in the various plots are maintained at their respective central value.

From Figure 2 it can be noted that the applied voltage has a significant effect on the MRR. An increase in the potential leads to an increase in the electrolyzing current as well as in the current density in the interelectrode gap involving a faster metal dissolution. This behaviour is found to be highly nonlinear and intensifies for the high voltage values.

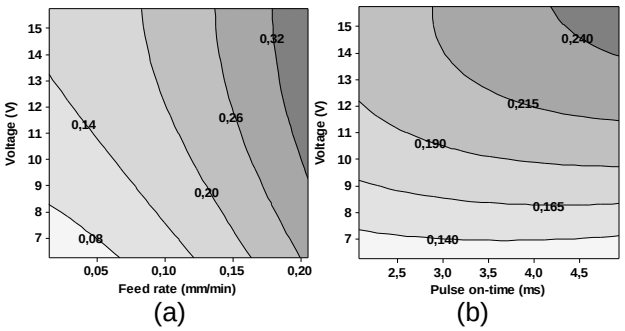

(a) (b)

Figure 2 - Effect of voltage and feed rate (a) and voltage and pulse on-time (b) on MRR (g/min)

This complies with the fundamental principles of metal removal in PECM [2], [5], [6].

Besides, Figure 2(a) depicts the same dependency between cathode feed rate and MRR. An increasing of the feed rate leads to a reduction of the interelectrode gap, causing a decrease in electrical resistance and thus an increase in current intensity.

Trial	X_1	X_2	X_3	X_4	X_5	MRR (g/min)	R_a (µm)
1	-1	-1	-1	-1	-1	0.1408	8.4169
2	1	-1	-1	-1	-1	0.1940	7.4627
3	-1	1	-1	-1	-1	0.1333	8.7564
4	1	1	-1	-1	-1	0.1989	8.1251
5	-1	-1	1	-1	-1	0.1485	8.3304
6	1	-1	1	-1	-1	0.1696	8.5364
7	-1	1	1	-1	-1	0.1554	8.2090
8	1	1	1	-1	-1	0.2214	9.4049
9	-1	-1	-1	1	-1	0.2370	4.9984
10	1	-1	-1	1	-1	0.2803	5.3894
11	-1	1	-1	1	-1	0.2394	5.4220
12	1	1	-1	1	-1	0.2729	6.3909
13	-1	-1	1	1	-1	0.2376	6.4883
14	1	-1	1	1	-1	0.2635	7.0447
15	-1	1	1	1	-1	0.2293	6.2233
16	1	1	1	1	-1	0.2807	7.2264
17	-1	-1	-1	-1	1	0.1406	7.8714
18	1	-1	-1	-1	1	0.1577	6.7409
19	-1	1	-1	-1	1	0.1458	9.0215
20	1	1	-1	-1	1	0.1908	8.4589
21	-1	-1	1	-1	1	0.1418	8.2347
22	1	-1	1	-1	1	0.1567	7.8132
23	-1	1	1	-1	1	0.1462	8.1232
24	1	1	1	-1	1	0.1929	9.0654
25	-1	-1	-1	1	1	0.2309	5.1497
26	1	-1	-1	1	1	0.2655	5.4764
27	-1	1	-1	1	1	0.2339	5.4657
28	1	1	-1	1	1	0.2600	6.2495
29	-1	-1	1	1	1	0.2417	5.4091
30	1	-1	1	1	1	0.2749	6.4814
31	-1	1	1	1	1	0.2370	5.6044
32	1	1	1	1	1	0.2837	7.3286
33	-α	0	0	0	0	0.1014	7.4218
34	α	0	0	0	0	0.2467	7.5354
35	0	-α	0	0	0	0.1761	6.0670
36	0	α	0	0	0	0.2092	7.5611
37	0	0	-α	0	0	0.2104	6.5481
38	0	0	α	0	0	0.2181	7.3005
39	0	0	0	-α	0	0.1102	11.0183
40	0	0	0	α	0	0.3428	6.2271
41	0	0	0	0	-α	0.2063	6.5932
42	0	0	0	0	α	0.1837	5.3641
43	0	0	0	0	0	0.2042	6.4439
44	0	0	0	0	0	0.1890	6.3256
45	0	0	0	0	0	0.2124	6.4511
46	0	0	0	0	0	0.1946	6.7252
47	0	0	0	0	0	0.1911	6.7806
48	0	0	0	0	0	0.1960	6.5417
49	0	0	0	0	0	0.2076	6.3573
50	0	0	0	0	0	0.2021	6.3723
51	0	0	0	0	0	0.2077	6.1478
52	0	0	0	0	0	0.1961	6.3460

Table 3 - Experimental design matrix and results

Source of variation	Degrees of freedom	Sum of squares		Mean sum of squares		F-value	
		MRR	R_a	MRR	R_a	MRR	R_a
Linear	5	0.115778	61.2485	0.023156	12.2497	218.94	162.69
Square	5	0.003799	11.6126	0.000760	2.3225	7.18	30.85
Interaction	10	0.000866	6.2741	0.000087	0.6274	0.82	8.33
Lack of fit	22	0.002725	2.0084	0.000124	0.0913	2.02	2.52
Error	9	0.000553	0.3257	0.000061	0.0362		
Total	51	0.123721	81.4694				

Table 4 - Analysis of variance for material removal rate (MRR) and surface roughness (R_a)

Levels of factors					Model		Experiment		$t_{calculated}$	
X_1	X_2	X_3	X_4	X_5	MRR (g/min)	R_a (µm)	MRR (g/min)	R_a (µm)	MRR	R_a
1	-1	0.5	0	-0.5	0.2095	6.8480	0.2179	6.8152	0.8186	0.1196
0.5	0.5	-1	-0.5	0	0.1912	7.2118	0.1959	7.2986	0.4601	0.3163
0	-0.5	1	0.5	1	0.2346	6.0145	0.2419	6.1388	0.7086	0.4529
0.5	0.5	0.5	0.5	0.5	0.2412	6.4992	0.2540	6.6808	1.2398	0.6617
-0.5	-0.5	-0.5	-0.5	-0.5	0.1604	7.0540	0.1711	7.2111	1.0424	0.5725

Table 5 - Confirmation student's *t*-test results for MRR and R_a

Moreover, Figure 2(b) illustrates the influence of applied voltage and pulse on-time on MRR. At low potential, pulse on-time does not significantly influence MRR. This can be explained by the fact that at low potential, i.e. low current density, also the material removal efficiency is low [1] and the current is primarily used to produce oxygen bubbles. Therefore, a longer pulse on-time principally causes more gas formation. At higher voltage values, the efficiency increases [1] and a longer pulse on-time implies more exchange of electric charges, i.e. more anodic dissolution.

Figure 3(a) exhibits the variation of MRR with respect to pulse on-time and electrolyte pressure. The MRR rises with high pressure. At high pressure, the removal products evacuation from the interelectrode gap is promoted and the gas bubbles growth on the electrodes is repressed, ensuring better electrolyte conductivity and thus better material dissolution. At very high pressure values a mechanism of mechanical erosion is taking place parallel to those of diffusion and migration. The inert graphite particles, once dislodged from the ferritic or perlitic matrix, hammer and deteriorate the electrode surface [6]. This mechanism becomes increasingly severe with higher pressure. At high pulse on-time and low pressure values, the MRR also increases. This can be attributed to the laminar flow condition improving the electrolyte refreshment.

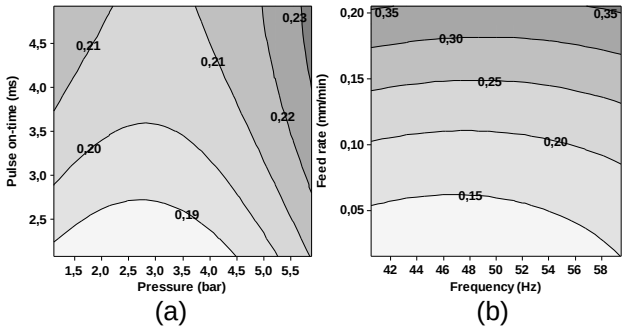

Figure 3 - Effect of pulse on-time and pressure (a) and feed rate and frequency (b) on MRR (g/min)

Figure 3(b) shows the influence of feed rate and vibration frequency. The material removal is not significantly influenced by the frequency but becomes higher at the extremes. As electrical impulses are triggered at each bottom dead centre, more electric charges, i.e. more dissolution, can be exchanged at high frequency. In contrast, at low frequency fewer pulses are generated but the electrolyte refresh in the interelectrode gap becomes more efficient, thus increasing the conductivity and therefore also the current density.

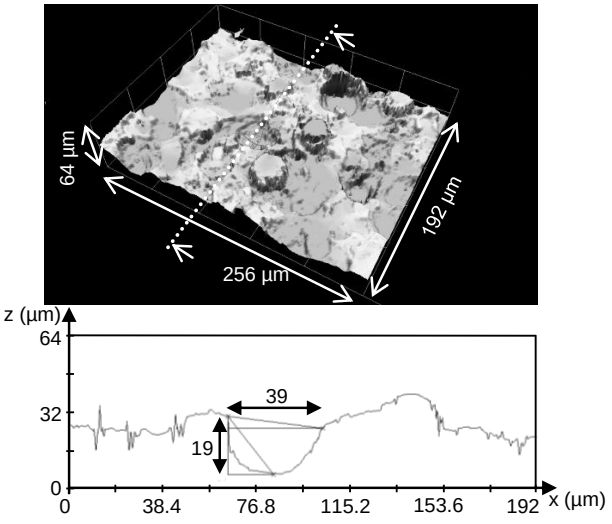

Figure 4 - Topography of a machined spheroidal cast iron surface at low voltage and low feed rate

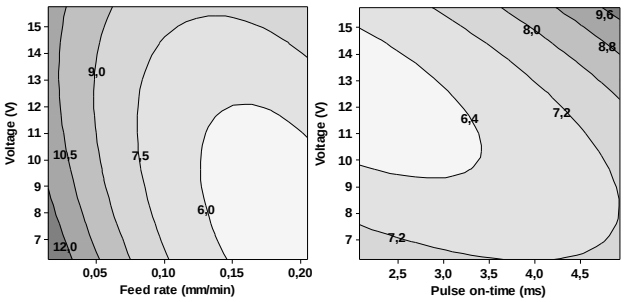

(a) (b)

Figure 5 - Effect of voltage and feed rate (a) and voltage and pulse on-time (b) on R_a (µm)

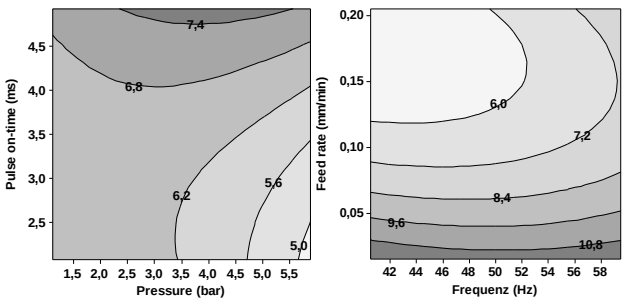

(a) (b)

Figure 6 - Effect of pulse on-time and pressure (a) and feed rate and frequency (b) on R_a (µm)

6.2 Effect of machining parameters on R_a

Based on Eq. (3) as developed through the experimental observations and response surface methodology, studies of the effects of various process parameters on the surface roughness were carried out to analyse the suitable parametric combinations that ensure controlled R_a effects. The contour plots - Figures 5 and 6 - show the effects for various parameter combinations. The numbers represented in the contour plots are R_a values.

Figure 5(a) illustrates the effect of applied voltage and feed rate on the surface roughness. At low voltage and low feed rate, the current density stays globally low at the anode surface but becomes locally amplified at the electrochemically preferred attack zones such as grain boundary [5], [6], [7] and especially graphite-iron interfaces [1]. The difference in electric conductivity between graphite and iron leads to an amplification of the local electrical field at their interface, implying a higher current density. Thus, the microstructure is inhomogeneously oxidized, leading to an extremely poor surface finish (Figure 4). High feed rates lead to a smaller interelectrode gap and thus a better copying accuracy and surface roughness. At the anode surface, a polish film grows, hindering the transport of metal ions so that the shortest diffusion path is privileged. This leads to a surface levelling [5].

Figure 5(b) exhibits the influence of applied voltage and pulse on-time on R_a. The surface integrity is improved for high voltages and short pulses on-time. High voltage values increase the current density and therefore the finish quality. At a short pulse on-time, the working gap decreases at constant feed rate, and therefore also the ohmic resistance. The result is an increased current density and consequently a better surface quality. At optimal pulse lengths, a polish film grows on the anode surface in which the ionic transport is hindered, involving a preferred metal dissolution at short diffusion paths leading to a surface levelling. If the pulse on-time is too short and the applied voltage is too low, i.e. low current density, the polish film cannot form. Inversely, at long pulse on-time - and particularly in addition at high voltage values - the polish film grows in a way that it perturbs the electrolyte flow by creating micro turbulences which reduce the levelling effect [5], [6].

Figure 6(a) shows the influence of pulse on-time and electrolyte pressure on R_a. The minimal surface roughness is obtained for high pressure and low pulse on-time. As explained before, a short pulse enables the optimal growth of a polish film at the anode surface, levelling the troughs and peaks, whereas long pulses cause such an important film growth that it interferes with the electrolyte flow, creating micro turbulence and thus diminishing the resulting surface finish [5]. At short pulse on-time, high pressure prevents the gas bubbles formation which leads to electrolyte disparities in the interelectrode gap and therefore inhomogeneous removal ratios. However, by triggering long impulses the pressure should be maintained at low values in order to avoid mechanical erosion.

Figure 6(b) indicates the influence of feed rate and cathode vibration frequency on R_a. At low feed rate values, i.e. low current density, the vibration frequency does not have a significant impact on surface roughness because the interelectrode gap is then large enough to ensure the electrolyte renewal. Yet, at a high feed rate and thus high current density and small interelectrode gap, a slow up and down cathode movement improves the flow condition through better removal products evacuation and electrolyte refreshment.

7 ANALYSIS FOR OPTIMISATION OF THE RESPONSES

Based on the developed second-order response surface equation, the behaviour and the evolution of the considered criteria can be predicted according to the various process parameters on the whole

Process parameters	Values obtained	
	MRR	R_a
Voltage (V)	15.8	13.5
Pulse on-time (ms)	4.9	2.1
Frequency (Hz)	59.5	40.5
Feed rate (mm/min)	0.205	0.157
Pressure (bar)	1.12	5.88

Table 6 - Optimal values of process parameters to maximize MRR or minimize R_a

domain of investigation. Thus, boundary values can be set for MRR and R_a to optimize the machining parameters in order to maximize the surface quality and to minimize the manufacturing time.

Those optimal parameter combinations for maximizing the MRR and minimizing the R_a value of various machined workpieces are determined by solving Eq. (2) and (3) using the software MINITAB. The optimal values of the process variables obtained for achieving controlled pulse electrochemical machining of workpieces within the bounds of the mathematical models have been listed in Table 6.

8 CONCLUSIONS

The analysis of the experimental observations using the Response Surface Methodology has demonstrated the dependence of the investigated criteria, namely material removal rate and surface roughness, and the PECM process parameters considered in the present study (applied voltage, electric pulse on-time, cathode vibration frequency, cathode feed rate and electrolyte pressure).

The mathematical models developed on the basis of RSM have been found to be very powerful to predict the complex, interactive and higher-order effects of the various predominant machining variables on the investigated criteria as demonstrated in the analysis of variance. Besides, these formulations will not only help in analyzing the influence of the predominant process parameters, but they are also useful for the optimal search of various parametric combinations for achieving a maximum and faster fulfilment of the objective requirements of controlled PECM in practical applications.

The present results are profitable for both design and production engineers to assess the necessary information about MRR and R_a in PECM processes to achieve beneficial operational performance and low experimental costs.

The effective and efficient use of PECM technology for machining spheroidal cast iron to achieve the optimal combination of an enhanced metal removal rate and the generation of necessary surface integrity has been attempted.

9 ACKNOWLEDGEMENT

The authors gratefully acknowledge the European Regional Development Fund and the program INTERREG IVa for the financial support.

10 REFERENCES

[1] Weber O.; Natter H.; Rebschläger A.; Bähre D., 2011, Surface quality and process behavior during Precise Electrochemical Machining of cast iron, Proceedings of the 7th International Symposium on Electrochemical Machining Technology, 41-46.

[2] Rajurkar K.P., Kozak J., Wei B., 1993, Study of pulse electrochemical machining characteristics, Ann. CIRP, 42/1:231-234.

[3] Bhattacharyya B., Sorkhel S.K., 2011, Investigation for controlled electrochemical machining through response surface methodology-based approach, J. Mater. Process. Technol., 86:200-207.

[4] Siebertz L., Van Bebber D., Hochkirchen T., 2010, Design of Experiments (DoE), Springer Heidelberg Dordrecht London New York.

[5] Moser S., 2004, Mikrostrukturierung von Metallen durch elektrochemischen Abtrag mit gepulstem Strom (PECM), PhD-Thesis, Heinrich Heine University Düsseldorf.

[6] Wagner T., 2002, High rate electrochemical dissolution of iron-based alloys in NaCl and $NaNo_3$ electrolytes, PhD-Thesis, University of Stuttgart.

[7] Senthilkumar C., Ganesan G., Karthikeyan R., 2009, Study of electrochemical machining characteristics of Al-SiC_p composites, Int. J. Adv. Manuf. Technol., 43:256-263.

11 BIOGRAPHY

Olivier Weber obtained his master degree in Mechanical Engineering from both the Arts et Métiers ParisTech (France) and the Karlsruhe Institute of Technology (Germany). He is currently doctoral fellow at the Institute of Production Engineering at Saarland University and research engineer at the Center for Mechatronics and Automatization.

Dirk Bähre obtained his PhD degree in Production Engineering from the Technical University of Kaiserslautern. In 2008 he was appointed Professor in Production Engineering at Saarland University, Germany.

Andreas Rebschläger obtained his master degree in Mechatronics from Saarland University. He is currently doctoral fellow at the Institute of Production Engineering at Saarland University and research engineer at the Center for Mechatronics and Automatization.